Transferable tight-binding models for silicon

I. Kwon
Group T-4, MS B268, Los Alamos National Laboratory, Los Alamos, New Mexico 87545

R. Biswas, C. Z. Wang, K. M. Ho, and C. M. Soukoulis
Ames Laboratory, Microelectronics Research Center and Department of Physics and Astronomy, Iowa State University, Ames, Iowa 50011
(Received 26 October 1993)

A transferable tight-binding model for silicon is found by fitting the energies of silicon in various bulk crystal structures and examining functional parametrizations of the tight-binding forms. The model has short-range radial forms similar to the tight-binding Hamiltonian of Goodwin, Skinner, and Pettifor but can be utilized in molecular dynamics with a fixed radial cutoff for all structural configurations. In addition to a very good fit to the energy of Si in different bulk crystal structures the model describes very well the elastic constants, defect-formation energies for vacancies and interstitials in crystalline silicon, the melting of Si, and short-range order in liquid silicon. Results for phonon frequencies and Grüneisen constants in *c*-Si are also presented.

I. INTRODUCTION

An outstanding problem in the computer-based microscopic description of materials, especially for molecular dynamics of semiconductor materials, is the need for an accurate transferable model of the energetic and electronic properties of semiconductor structures. Classical potential models[1–4] have been extensively developed either by fitting to *ab initio* calculations for Si or through other empirical means. These classical models have had much success in describing melting of silicon,[1] amorphous silicon structures, thin-film growth, and a variety of computationally intensive molecular-dynamics simulations.[4] However, by their very nature, the classical-based models do not contain important electronic information which is essential in a variety of problems such as determining the gap states for structural defects. Electronic-driven effects such as a Jahn-Teller distortion at a vacancy are specifically not described in classical molecular-dynamics models. The accuracy of the classical models in very distorted configurations, far from the fitting database, is also uncertain.

At the other extreme molecular-dynamics simulations based on the Car-Parrinello method[5] using the local-density approximation have been very successful in dealing with melting of silicon and amorphous structures.[6] While being very accurate and yielding much valuable electronic information, the *ab initio* molecular dynamics has been performed on small systems (~ 100 atoms) for short-time scales (~ 10 ps). Both larger systems and longer times scales are needed for understanding complex dynamical processes such as the those involved in growth and epitaxy. The development of *ab initio* electronic structure methods that scale linearly with the number of atoms and could be applied to large systems is an area of much current effort.

In this paper we aim to find tight-binding models for silicon that are in between the *ab initio* simulations and the classical models for molecular dynamics in level of sophistication. Our goal is to describe accurately the electronic and structural properties with tight-binding models but still have models robust enough for pursuing long-time simulation on large systems with a few hundred atoms. The tight-binding method has been very popular in many studies of silicon surfaces and defects, but has not always been very transferable to general geometries. In this paper we demonstrate that transferable tight-binding models for silicon can be found by careful fitting of *ab initio* calculations and exploring the large parameter space of tight-binding parameters. As will be demonstrated, these tight-binding models are in many cases comparable in accuracy to *ab initio* calculations.

II. TIGHT-BINDING MODELS FOR SILICON

In the tight-binding molecular-dynamics (TBMD) scheme, the Hamiltonian governing the atomic motions for $N_{\rm at}$ atoms is

$$H=\sum_i \frac{Pi^2}{2m}+\sum_n \langle \Psi_n|H_{\rm TB}|\Psi_n\rangle+E_{\rm rep}+E_0N_{\rm at} \ . \quad (1)$$

The first term is the kinetic energy of the ions, the second term is the electronic energy calculated by summing eigenvalues of filled states from a tight-binding Hamiltonian $H_{\rm TB}$, and $E_{\rm rep}$ is a repulsive potential representing the ion-ion repulsion and correcting for the double counting of the electron-electron interaction of the second term. E_0 is a constant energy shift per atom.

In early approaches, Chadi[7] used the minimal basis of s and three p orbitals per silicon atom and enforced a $(1/d^2)$ dependence[8] of the tight-binding hopping matrix elements with bond length d. The atomic energies E_s, E_p, and strengths of the hopping matrix elements $Vss\sigma$, $Vsp\sigma$, $Vpp\sigma$, and $Vpp\pi$ were inferred from fits to the silicon band structure. The parameters of the repulsive pair

 ©1994 The American Physical Society

potential were extracted by fitting to the crystal-silicon lattice constant and bulk modulus.[9] This approach was very successful in dealing with small distortions of c-Si and surface reconstructions on Si(100). By an alternative method of fitting $\phi(r_{ij})$ to local-density approximation (LDA) calculations of the total energy of silicon[10] as a function of bond length, this model provided accurate anharmonic properties such as temperature-dependent phonon frequency shifts and phonon linewidths,[11] and thermal expansion of Si.[12]

While this approach is very successful in a variety of applications, it is difficult to perform molecular dynamics with the slow $1/d^2$ scaling of TB matrix elements. The values of the matrix elements are non-negligible near the second-neighbor distances in silicon, yet incorporation of neighbors other than the first-neighbor shell in c-Si would lead to inaccuracies. This implies using a cutoff r_c between the first- and second-neighbor distances,[13] although the values of the TB matrix elements $h(r_{ij})$ and $\phi(r_{ij})$ would be nonzero at this cutoff. This discontinuity in the Hamiltonian at r_c would be impractical for molecular dynamics of general structural configurations. Another difficulty with this approach is its transferability to structural configurations that are very different from diamond structure c-Si, especially the need to model the phase diagram of silicon and defect energies in c-Si with the same parameter set.

A very important development toward both of these problems was made by Goodwin, Skinner, and Pettifor,[14] who proposed short-range scaling functions

$$h_\alpha(r)=h_\alpha(r_0)\left[\frac{r_0}{r}\right]^n \times\exp\left\{n\left[-\left[\frac{r}{r_c}\right]^{n_c}+\left[\frac{r_0}{r_c}\right]^{n_c}\right]\right\}, \quad (2)$$

$$\phi(r)=\phi(r_0)\left[\frac{r_0}{r}\right]^m \times\exp\left\{m\left[-\left[\frac{r}{r_c}\right]^{n_c}+\left[\frac{r_0}{r_c}\right]^{n_c}\right]\right\}. \quad (3)$$

Here $h_\alpha(r)$ represents the distance-dependent tight-binding overlaps, with α denoting the four tight-binding overlaps ($ss\sigma$, $sp\sigma$, $pp\sigma$, and $pp\pi$). The atomic interactions are short ranged and decay more rapidly than simple exponentials. r_c controls the range of the interactions, and n_c and m_c the decay of the scaling forms. r_0 is the nearest-neighbor separation in the equilibrium diamond structure. Goodwin, Skinner, and Pettifor found values of $n=2$ and $m=4.54$. The parameters of this model were found[14] by fitting to the phase diagram of silicon including energy as a function of bond length for diamond, and fcc structures from first-principles local-density approximation (LDA) calculations.

The Goodwin, Skinner, and Pettifor[14] model reproduced the bulk phase energies of silicon [Fig. 1(b) of Ref. 15] when the TB parameters were restricted to the first-neighbor shells of all the structures.[15] However, it is impossible to choose a unique cutoff distance that satisfies the condition that all crystalline structures of Si have only nearest-neighbor interactions. When this model is used for simulating a liquid a unique cutoff distance is required, which was found to be about 3.60 Å—a value between the first- and second-neighbor distances of the diamond structure. This choice of cutoff does not alter the energy curve of diamond [Fig. 1(c) of Ref. 15]. However, when we do use this cutoff distance of 3.60 Å, notable effects are found on the metallic structures which are shifted to higher-energy values. The phase diagram [Fig. 1(c) of Ref. 15] becomes significantly poorer.

III. DEVELOPMENT OF NEW TIGHT-BINDING MODEL

In this paper we address the problem of model of Goodwin, Skinner, and Pettifor by examining alternative scaling forms that can be used with a single unique cutoff in molecular dynamics that provides a good phase diagram for silicon.

We have used the scaling form for the TB matrix element

$$h_\alpha(r)=h_\alpha(r_0)\left[\frac{r_0}{r}\right]^n \times\exp\left\{n\left[-\left[\frac{r}{r_{c\alpha}}\right]^{n_{c\alpha}}+\left[\frac{r_0}{r_{c\alpha}}\right]^{n_{c\alpha}}\right]\right\}. \quad (4)$$

Here, α denotes the four tight-binding overlaps. The two-body energy is a sum of a functional f of the repulsive pair potential $\phi(r_{ij})$, similar to expressions in the embedded-atom approach and in recent TB models of carbon,[16] and is given by

$$E_{\rm rep}=\sum_i f\left[\sum_j \phi(r_{ij})\right], \quad (5)$$

$$f(x)=C_1x+C_2x^2+C_3x^3+C_4x^4, \quad (6)$$

$$\phi(r)=\left[\frac{r_0}{r}\right]^m \times\exp\left\{m\left[-\left[\frac{r}{d_c}\right]^{m_c}+\left[\frac{r_0}{d_c}\right]^{m_c}\right]\right\}. \quad (7)$$

Our basic strategy was to start with the Goodwin, Skinner, and Pettifor (GPS) tight-binding model and allow greater functional freedom to provide a better fit to the bulk silicon crystal structures and to model better defect energies. For each set of tight-binding parameters (h_α, $n_{c\alpha}$, $r_{c\alpha}$, and n) the energies of the bulk phases of silicon were fitted with a nonlinear least-squares fitting routine to extract values for the two-body functional parameters (m, m_c, d_c, and C_i). The resulting tight-binding model was tested for elastic constants, phonon frequencies, Gruniesen constants, and defect formation energies (vacancy and interstitial energies).

We then examined variations of the tight-binding parameter set h_α, $n_{c\alpha}$, $r_{c\alpha}$, and n. We first considered the requirement that the s-wave function is shorter ranged than the p-wave function, implying a successively increasing range of the overlaps $ss\sigma$, $sp\sigma$, $pp\sigma$, and $pp\pi$. We

modeled this requirement by having a higher value of $n_{c\alpha}$ and a lower value of $r_{c\alpha}$ for $ss\sigma$ and $sp\sigma$ than the $pp\sigma$ and $pp\pi$ overlaps, which we took to have the same radial functions.

We then varied by small amounts values for each of the tight-binding overlap strengths $h_\alpha(r_0)$ for the $ss\sigma$, $sp\sigma$, and $pp\sigma$, and $pp\pi$ overlaps and the s-p energy splitting E_s-E_p. Only a single parameter was changed at one time and the fits were redone. If improvements were found, were found, another value of the electronic tight-binding parameter was adopted and the variation of the next parameter was considered. We found this strategy to be especially important in improving defect energies and maintaining the correct ordering of these defect energies. The tight-binding model parameters for our best fit are displayed in Table I, with the radial dependence of the overlaps plotted in Fig. 1. The repulsive pair potential $\phi(r)$ and the embedding energy $f(x)$ for our model are plotted in Fig. 2. We found that maintaining the same value of n ($n=2$) was necessary for physically reasonable results.

In addition to the GSP functional form [Eqs. (4) and (7)], we attempted a limited exploration of the large space of functional forms possible for the tight-binding overlaps. One such form enforced the condition that the $sp\sigma$ and $pp\sigma$ interactions should not be infinitely strong at short distances, but should saturate and approach constants at short distances. We used simple algebraic functions[17] that enforced this behavior instead of the $(r_0/r)^n$ polynomial in the tight-binding overlaps. Such functional forms provided accurate phonon frequencies together with a good fit of the phase diagram, but revealed negative or unphysically small Gruneisen parameters and were consequently not considered for further work.

We note that a different family of radially decaying functions (of the form $[1+\exp(r-r_c)/\mu]^{-1}$) has been developed in a tight-binding model by Sawada.[18] A modified version of Sawada's method has also been proposed by Kohyama.[19] A related functional form has also been employed by Mercer and Chou for tight-binding models of Si and Ge.[20]

TABLE I. Parameters for the silicon tight-binding model as defined in Eqs. (4)–(7). $r_0=2.360\,352$ Å, $n=2$, $E_s=-5.25$ eV, $E_p=1.20$ eV, and $E_0=8.739\,320\,4$ eV.

(a) Electronic parameters

α	$ss\sigma$	$sp\sigma$	$pp\sigma$	$pp\pi$
$h_\alpha(r_0)$ (eV)	−2.038	1.745	2.75	−1.075
n_c,α	9.5	8.5	7.5	7.5
r_c,α (Å)	3.4	3.55	3.7	3.7

(b) Two-body parameters

m	6.875 5
m_c	13.017
r_c (Å)	3.669 95
C_1 (eV)	2.160 438 5
C_2 (eV)	−0.138 439 3
C_3 (eV)	$5.839\,842\,3\times10^{-3}$
C_4 (eV)	$-8.026\,357\,7\times10^{-5}$

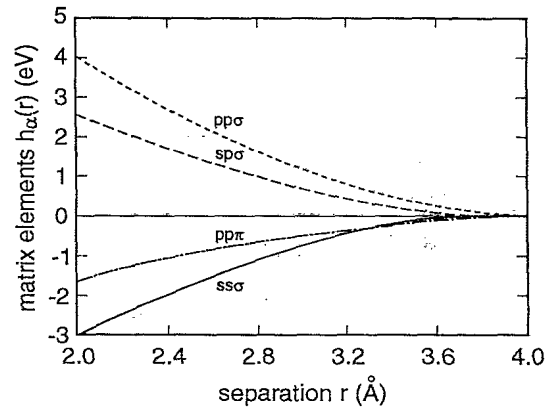

FIG. 1. Radial dependence of the tight-binding hopping matrix elements as a function of separation, as described by Eq. (4).

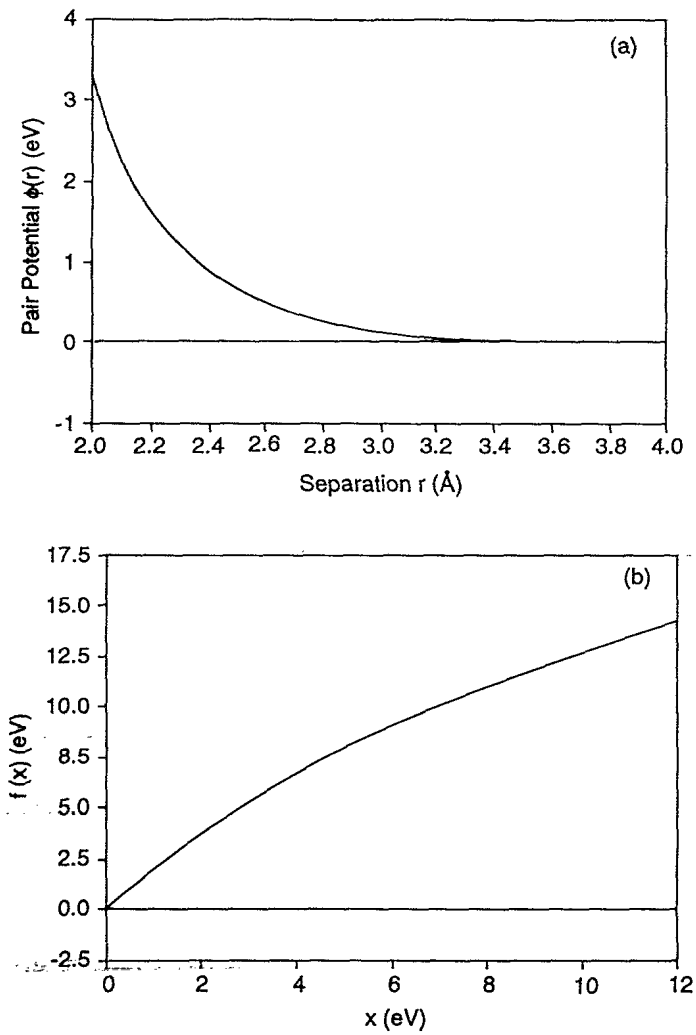

FIG. 2. (a) Radial dependence of the repulsive pair potential $\phi(r)$ as a function of separation r between atoms, as given by Eq. (7). (b) The embedding energy function $f(x)$ plotted as a function of x [Eq. (6)]. x is the sum of the pair potentials from the neighbors of an atom [Eq. (5)].

IV. RESULTS

The best-fit tight-binding model of Table I provided the bulk crystal structures of silicon (Fig. 3) which displays very good agreement with the LDA calculations for diamond and the metallic phase energies and bond lengths. The bulk moduli of the metallic phases is also reproduced very well. Although not shown in Fig. 3, wurtzite is about 0.02 eV above the diamond energy. Generally, the fit to the phase energies exceeds the quality of the fit from classical models.

In calculations of the phase diagram (Fig. 3) there is no ambiguity in the number of neighbor shells to be included as in the previous model[14] that used only the first-neighbor shell. All neighbor shells up to a distance of 4.16 Å were automatically included for the structural energies. As used in recent TB models of carbon[16] and for the convenience of molecular dynamics, we require the scaling function $h_\alpha(r)$ and potential $\phi(r)$ to go smoothly to zero at the designated cutoff distance $r_{\max}$ with a cubic polynomial:

$$\phi(r)=b_0+b_1(r-r_1)+b_2(r-r_1)^2+b_3(r-r_1)^3 \quad \text{for } r_1<r<r_{\max} \qquad (8)$$

with similar expressions for the scaling functions $h_\alpha(r)$. The four coefficients in (8) are determined by requiring that $\phi(r)$ go smoothly to zero at the cutoff distance $r_{\max}$ (4.16 Å), and that the $\phi(r)$ function in (8) smoothly join the scaling form (7) at the distance r_1 (4.0 Å). Alternatively, a fixed truncation of the functions between 4.1 and 4.2 Å produces similar results as using (8).

In addition to the range of structural geometries contained in the bulk silicon crystal structures, it is necessary to extensively test the tight-binding model for as many physical quantities for which experimental or *ab initio* results are known, to ensure the transferability of this model to any general structural geometry. For this purpose we have tested the tight-binding model for elastic constants, phonon frequencies, and Gruniesen constants of diamond silicon (Table II), and energies of defects in various sized supercells (Table III), including comparisons with LDA, experiment, and available results from the Stillinger-Weber classical Si model.[1]

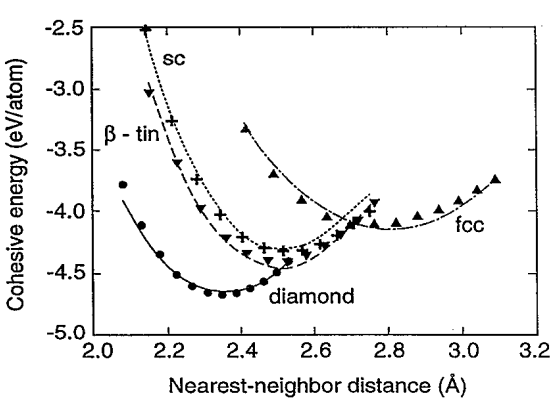

FIG. 3. Cohesive energy as a function of nearest-neighbor distance for several bulk phases of Si. The points are the LDA calculations (Ref. 10), and lines are from the present tight-binding model.

TABLE II. Values of the bulk modulus, elastic constants, phonon frequencies, and Gruneisen parameters of *c*-Si calculated with the present tight-binding Si model (TB), local-density-functional calculations (LDA), and the Stillinger-Weber Si potential (SW), compared to experimental results (Expt).

	TB	LDA	SW	Expt.
B (10^{11} erg/cm^3)	8.76	9.20	10.14	9.78
$C_{11}-C_{12}$ (10^{11} erg/cm^3)	9.39	9.80	7.50	10.12
C_{44}^0 (10^{11} erg/cm^3)	19.85	11.10		
C_{44} (10^{11} erg/cm^3)	8.90	8.50	5.64	7.96
$\nu_{\mathrm{LTO}(\Gamma)}$ (THz)	21.50	15.16	17.83	15.53
$\nu_{\mathrm{TA}(X)}$ (THz)	5.59	4.45	5.96	4.49
$\nu_{\mathrm{TO}(X)}$ (THz)	20.04	13.48		13.90
$\nu_{\mathrm{LOA}(X)}$ (THz)	14.08	12.16		12.32
$\gamma_{\mathrm{LTO}(\Gamma)}$	0.81	0.92	0.80	0.98
$\gamma_{\mathrm{TA}(X)}$	−0.51	−1.50	−0.04	−1.40
$\gamma_{\mathrm{TO}(X)}$	0.90	1.34	0.89	1.50
$\gamma_{\mathrm{LOA}(X)}$	0.61	0.92	0.83	0.90

Tables II and III illustrate the strengths and possible limitations of our present model. Elastic constants agree very well with experimental values to within a 12% accuracy. The present model is a distinct improvement over the Chadi model, which had soft elastic constants ($C_{11}-C_{12}=7.1, C_{44}^0=10.19$ and $C_{44}=6.17$, in units of 10^{11} erg/cm^3 for the Chadi model). Our value for the C_{44} elastic constant, including internal strain rearrangement, is particularly notable.

A limitation on the present model is that the phonon frequencies for the optic mode [LTO(Γ) and TO(X)] are 35–45 % higher than experimental values. This arises from the steep slope of the two-body potential at the equilibrium diamond bond length which is a measure of the bond stretching force constant. The high value of $m=6.8755$ in the two-body part leads to artificially high optic mode frequencies. In contrast, the Chadi model with $m=2$ has 16.95 THz for LTO(Γ) and the GSP model with $m=4.54$ has 18.31 THz for LTO(Γ), illustrating the trend with the m parameter.

It appears that globally modeling the energies of a wide variety of structural geometries, with a range of bond

TABLE III. Calculated formation energies for point defects in *c*-Si with the present tight-binding model for 64- and 216-atom supercells, compared with values from first-principles local-density-approximation (LDA) results. The values in the parentheses are formation energies of unrelaxed defects. All energies are in eV. T and H refer to the tetrahedral and hexagonal interstitial. The split interstitial was along the 110 axis.

Defect	64 atoms	216 atoms	LDA
Vacancy	3.46(4.72)	3.93(5.57)	3.6–4.1
T interstitial	3.61(4.12)	4.42(4.91)	4.3–6.2
H interstitial	4.75(5.92)	5.13(6.36)	5.0–6.0
Split interstitial	3.52(4.24)	3.84(4.71)	3.3

lengths and coordinations, is not fully compatible with accurately modeling some of the local properties of the diamond silicon structure. We anticipate that the present tight-binding model will not be used for calculations of phonons for which several other suitable models such as the Chadi model[7] and Keating force-constant model[21] are available. Instead we anticipate using the present tight-binding model for general molecular dynamics of silicon for which several of the previous tight-binding models were inadequate. As described in Sec. V, the melting properties are not dependent on this stiff optic mode frequency.

The acoustic-phonon branch is much better represented in the present model than the optic branch. The elastic constants and bulk modulus are directly related to the acoustic branch rather than the optic modes. The Gruneisen parameters (Table II) are all systematically smaller than experiment, but have the right relative magnitudes and produce the negative Gruneisen parameter for the TA(X) mode.

Important criteria in transferability of the tight binding models are the formation energies of vacancies and interstitials (Table III). All the defect formation energies require larger supercells, indicative of the long-range structural relaxations involved. A particularly notable feature is the prediction of LDA calculations[22,23] that the split interstitial defect is the lowest energy defect, a feature reproduced by our model (for the $N=216$ atom supercell). The split interstitial may be the most favored native defect in Si,[22,23] and consists of a pair of two bonded silicon atoms, oriented along the 110 direction, occupying a single lattice site.[24] The bond lengths at the split interstitial are substantially distorted from c-Si with approximately four bonds for the atoms of the pair (2.37, 2.40, 2.48, and 2.48 Å) somewhat longer than the 2.36 Å bond length for the ideal diamond structure. The $N=64$ atom supercells appear poorly converged (Table III) due to two sources of inaccuracy: (i) poor k-point sampling, since we only use $k=0$ in the calculation of electronic energies; and (ii) the interaction between defect levels in the finite-size periodic supercells. Both sources of inaccuracy are reduced for larger cells. In fact, defect formation energies previously calculated with the GSP model[25] showed little difference between 512- and 216-atom supercells, suggesting that the present 216-atom defect formation energies should reasonably be converged.

The increasing energies of the vacancy, T interstitial and H interstitial agrees well with the LDA values. The vacancy energy shown in Table III includes a small Jahn-Teller distortion that leads to pairing of atom pairs around the vacancy, and an energy lowering of about 0.02 eV from the symmetrically relaxed vacancy structure. In all the interstitial structures, there is a range of neighbor distances between 2.7 and 3.5 Å, between the first- and second-neighbor shells of diamond. Such neighbor distances are present in the metallic phases indicating an implicit relationship between the structures of the Si-phase diagram and those at defects, and emphasizes the importance of modeling the Si-phase diagram correctly. For this tight-binding model, diamond structure has a minimum indirect gap of 0.78 eV occurring between Γ and L. The minimum of the conduction band occurs at the L point, as is common in several tight-binding models.[7] The direct gap at the zone center is 1.62 eV and is much larger than the indirect gap. The conduction bands are generally not well modeled by a superposition of atomic states but are more free-electron-like. However, the conduction-band properties or unfilled states are less important for determining energies of bulk silicon structures.

V. MELTING OF SILICON

An important comparison of the tight-binding model with both experiment and *ab initio* calculations is then melting of silicon. Accordingly, we performed constant-volume and constant-temperature molecular-dynamics simulations on a 64-atom silicon cell with periodic boundary conditions (Fig. 4). The time step used was 1.07×10^{-15} s, and the density of the sample was set to the experimental density at the triple point, i.e., 2.53 g/cm^3.[26,27]

The simulation was initiated in the diamond-Si structure with the temperature raised in steps of about 300 K. At each temperature 1000 time steps are performed for equilibration of the configuration, followed by another 2000 time steps for calculation of the average energies and other statistical features of pair correlations and bond-angle correlations.

Due to the finite size of the cell and the short simulation time ($\sim$3.2 ps), there is a substantial superheating of the cell, and the crystal melts higher than the experimental temperature of 1685 K. Similarly, there is a substantial undercooling of the liquid. The liquid configuration at 2900 K was obtained on heating, whereas all the liquid configurations below 2900 K were obtained by successively cooling the 2900 K liquid configuration.

The shape of the solid and liquid curves agree well with those from other methods.[25] From the energy gap between the two branches we observe a latent heat of about 0.4 eV that is close to the experimental value of 0.47 eV at $T\approx1685$ K. From the slope of the total energy per atom of c-Si as a function of temperature (Fig. 4) we find

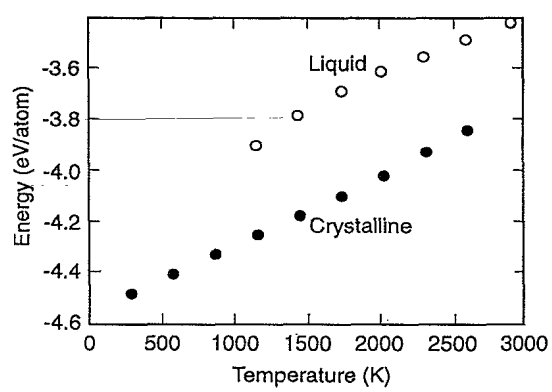

FIG. 4. Total energy (per atom) as a function of temperature for crystalline and liquid Si phases obtained by molecular dynamics with this tight-binding model. A 64-atom cell with periodic boundary conditions was used.

a specific heat per atom that is approximately $3k_B$, as would be expected for the classical limit above the Debye temperature of Si (625 K).

The calculated radial distribution function $g(r)$ for liquid silicon at 1740 K is compared with results from the *ab initio* Car-Parrinello simulation[6] in Fig. 5. To ensure greater statistical accuracy, 20 000 steps of equilibration were performed at 2000 K, followed by 20 000 equilibration steps at 1740 K and 1000 more steps over which time averaged $g(r)$ and $g3(\theta)$ were computed over 40 configurations for Figs. 5, 6, and 7. The position of the first peak of $g(r)$ (2.57 Å) is slightly larger than the Car-Parrinello result. The Car-Parrinello $g(r)$ is shifted toward smaller separation, partly because the liquid was at higher density (2.59 $\mathrm{g\,cm^{-3}}$) compared to our TBMD density of 2.53 $\mathrm{g\,cm^{-3}}$. Overall the TBMD $g(r)$ is narrower and larger in peak height than the Car-Parrinello result. The larger number of neighbors at short separations ($r<4.5$ a.u.) in Car-Parrinello is compensated for by a larger number of neighbors in the TBMD for larger separations (4.75 a.u. $<r<$ 5.25 a.u.) on the higher side of the first peak. The average nearest-neighbor distance in our simulation is 2.53 Å, compared with ~2.46 Å from the Car-Parrinello simulation,[6] 2.50 Å obtained by Virkkunen, Laasonen, and Nieminen,[27] and the experimental value of 2.50 Å.[28,29] The average number of neighbors within the first peak of $g(r)$ is ~6.47 for integration up to 3.1 Å, comparable to the Car-Parrinello result of 6.5 and the experimental value of 6.4.[28,29] Notably the coordination number in our model and experiment is substantially smaller than the 8.07 value predicted by the Stillinger-Weber (SW) potential,[1] and the value of 7.17 from the GSP model for liquid Si.[15]

The bond-angle distribution using bond-length cutoffs of 3.1 and 2.51 Å is shown in Fig. 6, together with a comparison of Car-Parrinello results. For the bond-length cutoff of 3.1 Å, corresponding to the first minimum of $g(r)$, the bond-angle distribution shows a broad peak around 90°–100° and a narrower peak at 50°–60°, with

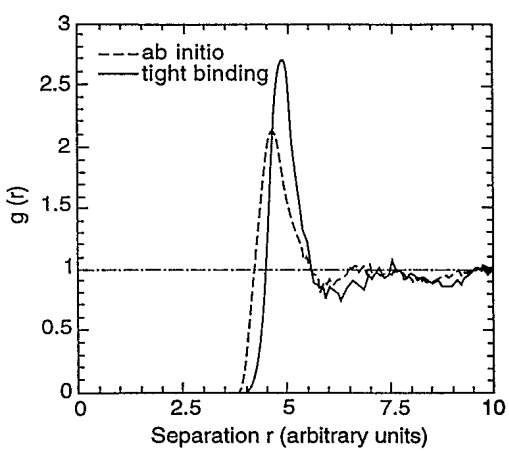

FIG. 5. Radial distribution function for liquid Si at $T=1740$ K. The thick line represents the present TBMD result. The broken line is the result from the Car-Parrinello method (Ref. 6). The TBMD results here and in Figs. 7 and 8 are an average of 40 configurations over 1000 time steps.

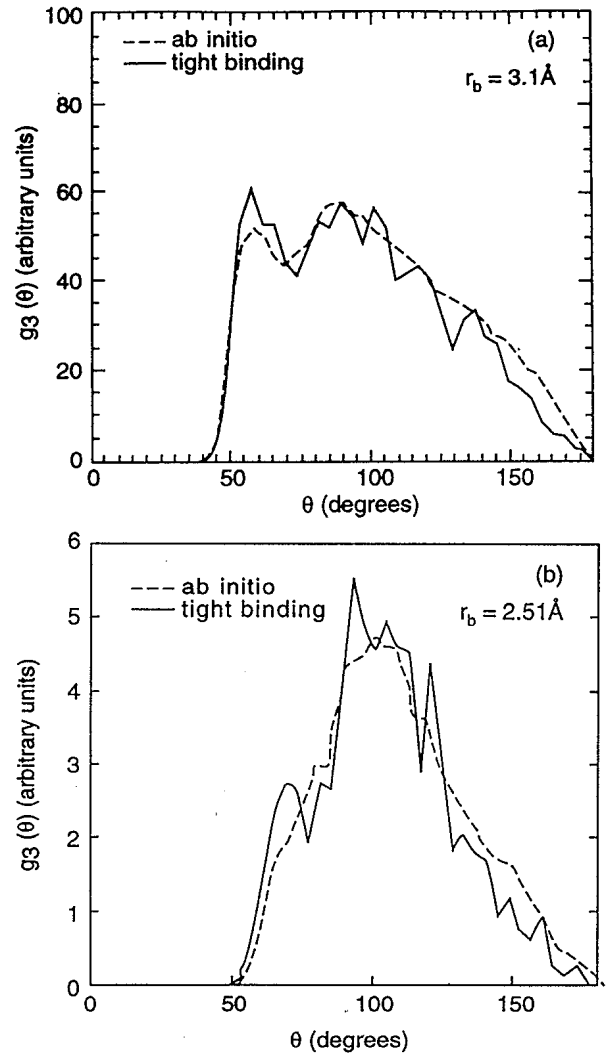

FIG. 6. Bond angle distribution functions $g_3(\theta)$ for liquid Si at $T=1740$ K for bond lengths less than 3.1 Å (r_b) [corresponding to the minimum of the $g(r)$ function in Fig. 5] in (a), and for bond lengths less than 2.51 Å (r_b) in (b). In both figures the thick lines are the result of the present TBMD simulation, and the broken lines are the *ab initio* Car-Parrinello results from Ref. 6.

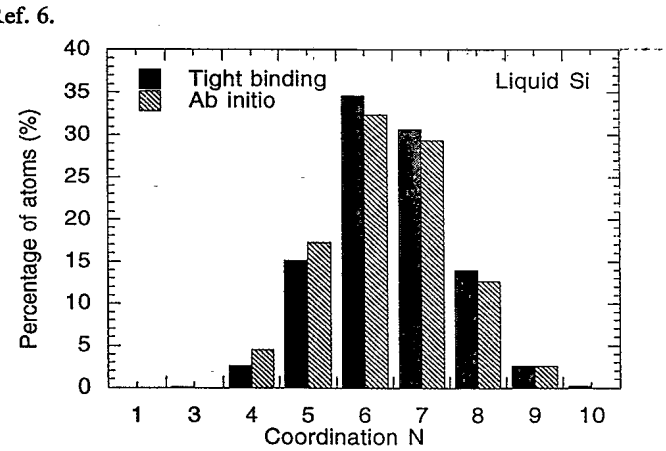

FIG. 7. The percentage of atoms with different coordinations for liquid Si at 1740 K with the present TBMD simulation, compared with the *ab initio* Car-Parrinello results from Ref. 6. In both cases a cutoff of 3.1 Å [corresponding to the first minimum of $g(r)$] was used to define the bonds.

very good agreement between the present TBMD and *ab initio*[6] results as illustrated in Fig. 6(a). This double-peak feature arises from the contribution of the tetrahedrallike bonding and the higher coordinated metallic bonding, respectively. Using a shorter cutoff of $r_b \sim 2.51$ Å reduces the strength of the 50°–60° peak supporting this interpretation of the 60° peak as arising from higher coordinated atoms with longer bond lengths. In both TBMD and *ab initio* results one is left with a broad feature peaking between 90° and 100°, as shown in Fig. 6(b), where the agreement between TBMD and *ab initio* methods also is very good. Notably the SW potential[1] fails to predict the second peak at 60°—a qualitatively different feature between classical simulations and the quantum-mechanical simulations of TBMD and *ab initio* methods.

The time-averaged coordination counts for TBMD and *ab initio* methods[6] for liquid Si are illustrated in Fig. 7, which shows a very good agreement for the distribution of atoms with different coordinations in both methods. The same cutoff bond length of 3.1 Å was used in both cases. TBMD provided an average coordination of 6.47 compared to 6.5 for *ab initio*.[6]

The TBMD simulations also provide information on the electronic properties for liquid Si (Fig. 8), a feature not present in classical model simulations. The absence of the gap in the electronic densities of states (Fig. 8), illustrates that liquid silicon is metallic.

The good agreement with liquid-Si properties indicate that the stiffer optic phonons do not play a crucial role in liquid-Si properties. Instead, the liquid properties and melting may depend more on the acoustic phonons, defect formation energies, and energies for bulk Si crystal structures.

VI. SILICON CLUSTERS

We have explored a limited number of small silicon cluster configurations to assess the applicability of the present TB model to silicon clusters. The small N-atom silicon clusters are a particularly stringent test since quantum-mechanical bonding effects dominate for $N \leq 10$ atoms. For N-atom Si clusters ($N \leq 5$) we have examined the lowest-energy configurations predicted by first-principles quantum-chemical calculations.[30,31] In all cases examined ($3 \leq N \leq 5$) the TB model agrees well with the lowest-energy configurations found from the *ab initio* calculations.[30,31] The cohesive energies are usually slightly lower than the *ab initio* results.

For Si_2, our TB model predicts a dimer with a bond length 2.45 Å and a cohesive energy 1.60 eV/atom. For Si_3, we found an isosceles triangle with a bond length 2.42 Å, an apex angle of 74.7° (Fig. 9), and a cohesive energy of 2.51 eV/atom to be the favored structure, in agreement with *ab initio* results. The linear chain had higher cohesive energy at 2.21 eV/atom. For Si_4, the lowest-energy configuration is a rhombus (Fig. 9) with four bonds at 2.48 Å, one bond at 2.56 Å and a cohesive energy of 3.21 eV/atom. In contrast, the tetrahedron and trigonal bipyramid had a lower cohesive energy of 2.83 eV/atom. For Si_5 we find that the trigonal bipyramid with cohesive energy 3.18 eV/atom to be favored, in agreement with *ab initio* results.[30,31] There are six bonds with a bond length 2.48 Å, whereas separations between base atoms are 3.59 Å, and those between the vertices are 2.74 Å. The square pyramid (3.13 eV/atom), pentagon (3.04 eV/atom), and tetrahedron (1.82 eV/atom) were found to be higher-energy configurations.

A general result is that the bond lengths of the clusters with the TB model are longer than those from *ab initio* calculations. The lowest-energy structures from the TB model agree well with the *ab initio* calculations,[30,31] sug-

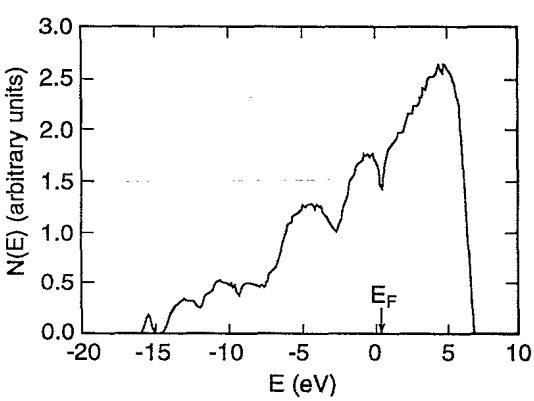

FIG. 8. Electronic densities of states for liquid Si at $T = 1740$ K for the present TBMD model.

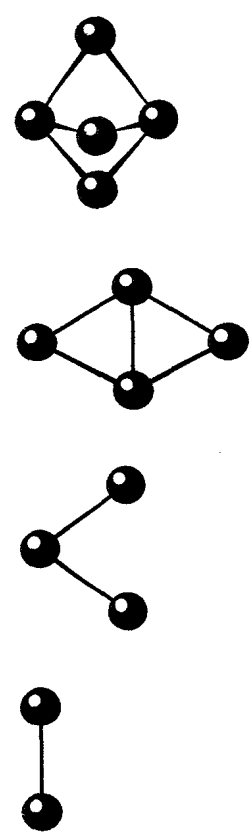

FIG. 9. Lowest energy structures found for N-atom silicon clusters for $N = 2$, 3, 4, and 5. The figures were computer generated. Bond lengths and cohesive energies of these structures are described in the text.

gesting that our tight-binding model could be utilized for further Si-cluster work. Simulated annealing of Si clusters is also an aspect for further work.

VII. CONCLUSIONS

We have developed a transferable tight-binding model for silicon that should be transferable to a wide range of structural geometries. The model was developed by fits to energies of the crystal structures of Si from first-principles LDA calculations by fitting short-range functions describing the tight-binding overlaps and repulsive potential. Different radial ranges are used for the $ss\sigma$, $sp\sigma$, and $pp\sigma$ (or $pp\pi$) interactions. The radial functions in the tight-binding model smoothly go to zero, enabling molecular-dynamics calculations to be performed without ambiguities of cutoffs present in earlier models. The energy of any structural configuration does not require a truncation of the model to a nearest-neighbor shell, but calculations over all neighbor pairs within the range of the model is necessary.

This tight-binding model for silicon reproduces very well the energies of different crystal structures for silicon, the elastic constants, and the formation energies of vacancies and interstitials in diamond-silicon. In good agreement with first-principles calculations, the model predicts that the split interstitial is the lowest-energy defect in crystalline silicon.

The melting of silicon has been simulated. There is good agreement for the latent heat at melting with the experiment value. The radial distribution function and the bond-angle distribution for liquid Si compare very well with *ab initio* Car-Parrinello simulations, including the prediction of a double-peak structure for the bond-angle distribution. Small Si clusters have been examined, and the low-energy configurations of Si_3, Si_4, and Si_5 agree well with *ab initio* calculations.

An underlying assumption of the tight binding model is the use of the minimal sp^3 basis. The validity of this assumption becomes weaker as we go down the group-IV column of C, Si, Ge, and α-Sn, and the energy gap decreases. The sp^3 basis set works very well for C, as illustrated by the very successful tight-binding models for C. In going to Si and then to Ge, the higher d states do come down in energy and lead to a small mixing into the filled valence-band states. This d-state contribution may be more important for the metallic higher coordinated crystal structures. While the sp^3 basis may work well in practice for Si, it may be much less adequate for Ge and certainly α-Sn. Investigation of d-state contributions is clearly an aspect for further work.

We anticipate the tight-binding model to be easily used in molecular-dynamics simulations, particularly for problems where electronic information is essential, including properties of amorphous structures, epitaxial growth, and surface diffusion.

ACKNOWLEDGMENTS

We thank C. H. Xu for assistance and for the use of a fitting program. We thank M. Y. Chou and J. Mercer for helpful discussions. We acknowledge support from the Electric Power Research Institute through the amorphous thin-film solar cell program and the Iowa Energy Center. This work is also supported by the Director of Energy Research, Office of Basic Energy Sciences and by the U.S. Air Force Office of Scientific Research. Ames Laboratory is operated for the U.S. Department of Energy by Iowa State University under Contract No. W-7405-ENG-82. Los Alamos National Laboratory is operated by the University of California under the auspices of the U.S. Department of Energy.

[1]F. Stillinger and T. Weber, Phys. Rev. B **31**, 5262 (1985).
[2]R. Biswas and D. R. Hamann, Phys. Rev. B **36**, 6434 (1987); Phys. Rev. Lett. **55**, 2001 (1985).
[3]J. Tersoff, Phys. Rev. Lett. **56**, 632 (1986); Phys. Rev. B **37**, 6991 (1988).
[4]I. Kwon, R. Biswas, G. S. Grest, and C. M. Soukoulis, Phys. Rev. B **41**, 3678 (1990).
[5]R. Car and M. Parrinello, Phys. Rev. Lett. **60**, 204 (1988).
[6]I. Stich, R. Car, and M. Parrinello, Phys. Rev. B **44**, 4262 (1991); Phys. Rev. Lett. **63**, 2240 (1989); Phys. Rev. B **44**, 11 092 (1991).
[7]D. J. Chadi, Phys. Rev. B **29**, 785 (1984).
[8]W. A. Harrison, *Electronic Structure and the Properties of Solids* (Freeman, San Francisco, 1980).
[9]D. J. Chadi and R. M. Martin, Solid State Commun. **19**, 643 (1976).
[10]M. T. Yin and M. L. Cohen, Phys. Rev. B **26**, 3295 (1982).
[11]C. Z. Wang, C. T. Chan, and K. M. Ho, Phys. Rev. B **42**, 11 276 (1990).
[12]C. H. Xu, C. Z. Wang, C. T. Chan, and K. M. Ho, Phys. Rev. B **43**, 5024 (1991).
[13]R. Biswas, C. Z. Wang, C. T. Chan, K. M. Ho, and C. M. Soukoulis, Phys. Rev. Lett. **63**, 1491 (1989).
[14]L. Goodwin, A. J. Skinner, and D. G. Pettifor, Europhys. Lett. **9**, 701 (1989).
[15]C. Z. Wang, C. T. Chan, and K. M. Ho, Phys. Rev. B **45**, 12 227 (1992).
[16]C. H. Xu, C. Z. Wang, C. T. Chan, and K. M. Ho, J. Phys. Condens. Matter **4**, 4047 (1992).
[17]The algebraic functions used were $r/(r^2+\varepsilon_1^2)^2$ and $r-\varepsilon_2/[(r-\varepsilon_2)^2+\varepsilon_2^2]^{3/2}$ for the $sp\sigma$ and $pp\sigma$ interactions.
[18]S. Sawada, Vacuum **41**, 612 (1990).
[19]M. Kohyama, J. Phys. Condens. Matter **3**, 2193 (1991).
[20]J. L. Mercer and M. Y. Chou, Phys. Rev. B **47**, 9366 (1993).
[21]P. N. Keating, Phys. Rev. **145**, 637 (1966).
[22]R. Car, P. Blochl, and E. Smargiassi, Mater. Sci. Forum **83-87**, 433 (1992).
[23]D. J. Chadi, Phys. Rev. B **46**, 9400 (1992).
[24]H. R. Schober, Phys. Rev. B **39**, 13 013 (1989).
[25]C. Z. Wang, C. T. Chan, and K. M. Ho, Phys. Rev. Lett. **66**, 189 (1991).
[26]A. R. Ubbelohde, *The Molten State of Matter* (Wiley, New

York, 1978), p. 239.
[27]R. Virkunnen, K. Laasonen, and R. M. Nieminen, J. Phys. Condens. Matter **3**, 7455 (1991).
[28]Y. Waseda and K. Suzuki, Z. Phys. B **20**, 339 (1975).
[29]J. P. Gabathuler and S. Steeb, Z. Naturforsch. Teil A **34**, 1314 (1979).
[30]K. Raghavachari and C. M. Rohlfing, J. Chem. Phys. **89**, 2219 (1988).
[31]R. Fournier, S. B. Sinott, and A. E. Depristo, J. Chem. Phys. **97**, 4149 (1992).